



## Degradation of tyrosine and tryptophan residues of peptides by type I photosensitized oxidation



Carolina Castaño<sup>a</sup>, Mariana Vignoni<sup>a</sup>, Patricia Vicendo<sup>b</sup>, Esther Oliveros<sup>b</sup>, Andrés H. Thomas<sup>a,\*</sup>

<sup>a</sup> Instituto de Investigaciones Físicoquímicas Teóricas y Aplicadas (INIFTA), Departamento de Química, Facultad de Ciencias Exactas, Universidad Nacional de La Plata, CCT La Plata-CONICET, Diagonal 113 y 64, 1900 La Plata, Argentina

<sup>b</sup> Laboratoire des Interactions Moléculaires et Réactivité Chimique et Photochimique (IMRCP), UMR 5623-CNRS/UPS, Université Toulouse III (Paul Sabatier), 118, route de Narbonne, F-31062 Toulouse cédex 9, France

### ARTICLE INFO

#### Article history:

Received 12 March 2016

Received in revised form 13 September 2016

Accepted 15 September 2016

Available online 16 September 2016

#### Keywords:

Pterins  
Electron transfer  
Photosensitization  
Tyrosine  
 $\alpha$ -MSH

### ABSTRACT

Pterin derivatives are involved in various biological functions, including enzymatic processes that take place in human skin. Unconjugated oxidized pterins are efficient photosensitizers under UV-A irradiation and accumulate in the skin of patients suffering from vitiligo, a chronic depigmentation disorder. These compounds are able to photoinduce the oxidation of the peptide  $\alpha$ -melanocyte-stimulating hormone ( $\alpha$ -MSH), which stimulates the production and release of melanin by melanocytes in skin and hair. In the present work we have used two peptides in which the amino acid sequence of  $\alpha$ -MSH was mutated to specifically investigate the reactivity of tryptophan (Trp) and tyrosine residues (Tyr). The parent compound of oxidized pterins (Ptr) was used as a model photosensitizer in aqueous solution at pH 5.5 and was exposed to UV-A radiation, a wavelength range where the peptides do not absorb. Trp residue yields N-formylkynurenine and hydroxytryptophan as oxidized products, whereas the Tyr undergoes dimerization and incorporation of oxygen atoms. In both cases, the first step of the mechanism involves an electron transfer from the amino acid to the photosensitizer triplet excited state, Ptr is not consumed and hydrogen peroxide ( $H_2O_2$ ) is released. The role of singlet oxygen produced by energy transfer from  $^3Ptr^*$  to dissolved  $O_2$  was negligible or minor. Other amino acid residues, such as histidine, might be also affected.

© 2016 Elsevier B.V. All rights reserved.

### 1. Introduction

Solar radiation induces modifications to different biomolecules and is implicated in the generation of human skin cancers [1]. Most of the solar UV energy incident on Earth surface corresponds to UV-A radiation (320–400 nm), which can induce damage through photosensitized reactions [2]. A photosensitized reaction is defined as a photochemical alteration occurring in one molecular entity as a result of the initial absorption of radiation by another molecular entity called photosensitizer [3]. Proteins and peptides are among the preferential targets of the photosensitized damaging effects of UV radiation on biological systems [4]. These processes may be mediated by endogenous or exogenous photosensitizers and can take place through different mechanisms: the generation of radicals (type I mechanism), e.g., via electron transfer or hydrogen abstraction, and the production of singlet oxygen ( $^1O_2$ ) (type II mechanism) [5].

In general, it is accepted that the photosensitization of proteins occurs mainly through the reactions of  $^1O_2$  with tryptophan (Trp), tyrosine (Tyr), histidine (His), methionine (Met) and cysteine (Cys)

side-chains [6]. However, we have recently demonstrated that the photosensitization of bovine serum albumin (BSA) by pterin (Ptr), the parent compound of oxidized (aromatic) pterins and an efficient  $^1O_2$  photosensitizer, involves a type I (electron transfer) mechanism [7,8]. In addition, in a series of studies performed in aqueous solution using free Trp [9], Tyr [10] and His [11] as target substrates and Ptr as a photosensitizer, we have demonstrated that in neutral and acidic media, a type I mechanism also predominates.

Pterins are present in human epidermis because 5,6,7,8-tetrahydrobiopterin ( $H_4Bip$ ) is an essential cofactor in the hydroxylation of the aromatic amino acids [12,13]. In vitiligo, a skin disorder characterized by a defective protection against UV radiation due to the acquired loss of constitutional pigmentation [14], the  $H_4Bip$  metabolism is altered [15] and unconjugated oxidized pterins accumulate in the affected tissues. These compounds are photochemically reactive in aqueous solution and, upon UV-A excitation, produce reactive oxygen species and photosensitize the oxidation of biomolecules [16].

In a recent work we have investigated the degradation of the  $\alpha$ -melanocyte-stimulating hormone ( $\alpha$ -MSH) photosensitized by Ptr under UV-A irradiation [17]. This peptide has the following amino acid sequence: Ac-Ser-Tyr-Ser-Met-Glu-His-Phe-Arg-Trp-Gly-Lys-Pro-Val. It stimulates the production and release of melanin by melanocytes in

\* Corresponding author.

E-mail address: [athomas@inifta.unlp.edu.ar](mailto:athomas@inifta.unlp.edu.ar) (A.H. Thomas).

skin and hair. When aerated solutions containing  $\alpha$ -MSH and Ptr (pH = 5.5) were exposed to UV-A radiation, the peptide was consumed and  $H_2O_2$  was generated, but without significant change in the photosensitizer concentration.

The photosensitization process is initiated by an electron transfer from  $\alpha$ -MSH to the triplet excited state of Ptr ( $^3\text{Ptr}^*$ ) yielding the peptide radical cation ( $\alpha\text{-MSH}^{\cdot+}$ ) and the Ptr radical anion ( $\text{Ptr}^{\cdot-}$ ) (Reaction (1)). The electron transfer from  $\text{Ptr}^{\cdot-}$  to  $O_2$  regenerates Ptr and forms superoxide anion ( $O_2^{\cdot-}$ ) (Reaction (2)), which, in turn, may disproportionate with its conjugated acid  $HO_2^{\cdot}$  to form  $H_2O_2$  (Reaction (3)). The radicals in the peptide react with  $O_2$  or other radicals to yield various products.



The present work was aimed at investigating specifically the reactivity and photoproducts of Trp and Tyr residues in peptides chains *via* a type I photosensitized process. For this purpose, we have used two peptides in which the amino acid sequence of  $\alpha$ -MSH was mutated (Scheme 1). In the peptide named  $\alpha$ -MSH<sub>W9G</sub>, the Trp residue in position 9 was mutated to a glycine (Gly), whereas in the peptide named  $\alpha$ -MSH<sub>Y2G</sub>, the Tyr residue in position 2 was mutated also to a glycine (Gly) residue. Aqueous solutions containing Ptr as a model photosensitizer and  $\alpha$ -MSH<sub>W9G</sub> or  $\alpha$ -MSH<sub>Y2G</sub> were exposed to UV-A radiation. Under the experimental conditions used, only Ptr was excited (Fig. 1). We focussed on the following specific objectives: i) characterization of the photoproducts formed by the oxidation of each residue; ii) corroboration of the hypothesis that the Tyr residue is responsible for the dimerization of the hormone  $\alpha$ -MSH; iii) elucidation of the reaction mechanisms.

## 2. Experimental

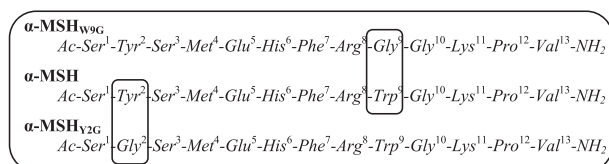
### 2.1. General

#### 2.1.1. Chemicals

Pterin (Ptr, purity > 99%, Schircks Laboratories, Switzerland) and the peptides ( $\alpha$ -MSH<sub>W9G</sub>, purity > 99.8%, and  $\alpha$ -MSH<sub>Y2G</sub>, purity > 99.1%, CASLO ApS, Denmark) were used without further purification after checking for impurities by HPLC. Acetonitrile (ACN) was purchased from J. T. Baker. Other chemicals were from Sigma Chemical Co. Solutions were prepared using deionized water further purified in a Milli Q Reagent Water System apparatus. The specific electrical resistance of water was  $\sim 10 \text{ M}\Omega \text{ cm}$ .

#### 2.1.2. Samples

All the experiments were carried out with aqueous solutions containing Ptr and a given peptide in the pH range 5.5–6.0, where Ptr is present at >99% in its acid form ( $pK_a$  7.9 [16]). For adjusting the pH of



**Scheme 1.** Molecular structures of  $\alpha$ -MSH and the modified peptides:  $\alpha$ -MSH<sub>W9G</sub> and  $\alpha$ -MSH<sub>Y2G</sub>, in which the Trp and the Tyr residues of  $\alpha$ -MSH were mutated to Gly residues, respectively.

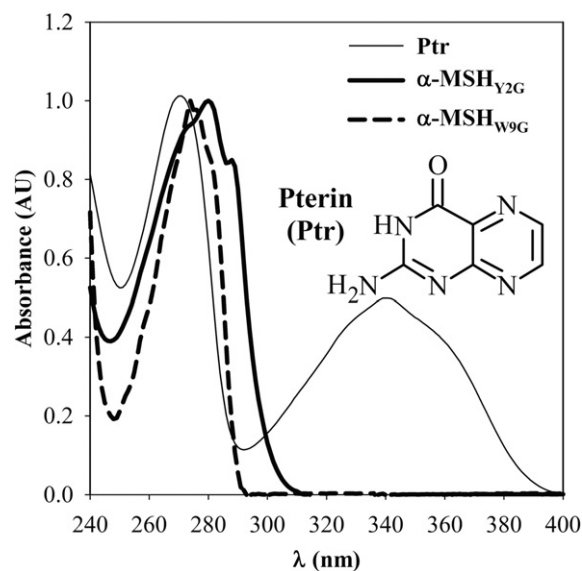


**Fig. 1.** Normalized absorption spectra of Ptr and the two peptides used in this work,  $\alpha$ -MSH<sub>W9G</sub> and  $\alpha$ -MSH<sub>Y2G</sub>, in air-equilibrated acidic (pH 5.5) aqueous solutions.

the solutions, small amounts of HCl or NaOH solutions (0.1–0.2 M) were added. The experiments were performed with air-equilibrated,  $O_2$ -saturated and  $O_2$ -free solutions. The two latter were obtained by bubbling for 20 min with  $O_2$  and Ar, respectively (Linde, purity > 99.998%).

#### 2.1.3. Estimation of the Concentration of the Peptides

It was assumed that the absorption of photons by  $\alpha$ -MSH<sub>W9G</sub> and  $\alpha$ -MSH<sub>Y2G</sub> at 280 nm is only due to the Tyr and Trp residues, respectively. It was also assumed that the molar absorption coefficient of the peptides at this wavelength are equal to the corresponding molar absorption coefficients of free Tyr and Trp in aqueous solutions at pH 5.5 ( $\epsilon_{\alpha\text{-MSH}_W9G}^{280} = \epsilon_{\text{Tyr}}^{280}$ ;  $\epsilon_{\alpha\text{-MSH}_Y2G}^{280} = \epsilon_{\text{Trp}}^{280}$ ). Therefore, the concentration of the peptide in each solution was estimated by determining the absorbance at 280 nm (before adding Ptr) and then using the Lambert-Beer law ( $A^{280} = \epsilon_{\alpha\text{-MSH}_W9G}^{280} l [\alpha\text{-MSH}_W9G]$ ;  $A^{280} = \epsilon_{\alpha\text{-MSH}_Y2G}^{280} l [\alpha\text{-MSH}_Y2G]$ ;  $l$  = optical pathlength).

#### 2.1.4. Steady-state Irradiation

Continuous photolysis experiments were carried out in quartz cells (1 cm optical path length) at room temperature. A Rayonet RPR lamp emitting at 350 nm (bandwidth  $\approx 20$  nm, Southern N.E. Ultraviolet Co., Branford, CT) was used as a radiation source. Under these experimental conditions only Ptr was excited (Fig. 1), whereas the peptides did not absorb radiation.

## 2.2. Analysis of Irradiated Solutions

### 2.2.1. UV/vis Spectrophotometric Analysis

Electronic absorption spectra were recorded on a Shimadzu UV-1800 spectrophotometer. Quartz cells (optical path length of 1 cm) were used for the measurements. The absorption spectra of the irradiated solutions were measured at regular time intervals.

### 2.2.2. High-performance Liquid Chromatography (HPLC)

A Prominence equipment from Shimadzu (solvent delivery module LC-20AT, on-line degasser DDU-20A5, communications bus module CBM-20, auto sampler SIL-20A HT, column oven CTO-10AS VP, photodiode array (PDA) detector SPD-M20A and fluorescence (FL) detector RF-20A) was employed for monitoring the photochemical processes. A Jupiter Proteo column (150  $\times$  4.6 mm, 4  $\mu\text{m}$ , Phenomenex) was used

for separation of the photosensitizer, the substrates and the products. The following mobile phases were used: 83% aqueous solution of ammonium acetate ( $\text{NH}_4\text{Ac}$ , 10 mM, pH 7) and 17% of ACN for  $\alpha\text{-MSH}_{\text{Y9G}}$ ; 80% aqueous solution of  $\text{NH}_4\text{Ac}$  (10 mM, pH 7) and 20% of ACN for  $\alpha\text{-MSH}_{\text{Y2G}}$ . In some cases, for further analysis, the products were isolated from HPLC runs (preparative HPLC), by collecting the mobile phase after passing through the PDA detector.

### 2.2.3. Detection and Quantification of $\text{H}_2\text{O}_2$

For the determination of  $\text{H}_2\text{O}_2$ , a Cholesterol Kit (Wiener Laboratorios S.A.I.C.) was used.  $\text{H}_2\text{O}_2$  was quantified after reaction with 4-aminophenazone and phenol [18,19]. Briefly, 500  $\mu\text{L}$  of irradiated solution were added to 600  $\mu\text{L}$  of reagent. The absorbance at 505 nm of the resulting mixture was measured after 30 min at room temperature, using the reagent as a blank. Aqueous  $\text{H}_2\text{O}_2$  solutions prepared from commercial standards were employed for calibration.

In all cases in which  $\text{H}_2\text{O}_2$  was detected and quantified, controls with catalase, the enzyme that catalyzes specifically the decomposition of  $\text{H}_2\text{O}_2$  to  $\text{H}_2\text{O}$  and  $\text{O}_2$ , were also carried out. Catalase was added after irradiation and before mixing the analyzed solution with the reactants. Thus, the absence of absorbance at 505 nm in these controls confirmed the presence of  $\text{H}_2\text{O}_2$  in the irradiated samples and excluded possible interferences of hydroperoxides formed on the amino acid residues.

### 2.2.4. Fluorescence Spectroscopy

Measurements were performed using a single-photon-counting fluorometer FL3 TCSPC-SP (Horiba Jobin Yvon). The equipment has been previously described in detail [20]. Briefly, the sample solution in a quartz cell was irradiated with a 450 W Xenon source through an excitation monochromator. The fluorescence, after passing through an emission monochromator, was registered at  $90^\circ$  with respect to the incident beam using a room-temperature R928P detector. Corrected fluorescence spectra obtained by excitation at 300 nm were recorded between 320 and 550 nm.

### 2.2.5. Mass Spectrometry Analysis

The liquid chromatography equipment/mass spectrometry system was equipped with an UPLC chromatograph (ACQUITY UPLC from Waters) coupled to a quadrupole time-of-flight mass spectrometer (Xevo G2-QToF-MS from Waters) (UPLC-QToF-MS). UPLC analyses were performed using the same column as for HPLC analysis and isocratic elution with 75% aqueous solution of  $\text{NH}_4\text{Ac}$  (10 mM, pH 7) and 25% of ACN at a flow rate of  $0.2 \text{ mL min}^{-1}$ . The samples were injected in the chromatograph, the components were separated and then the mass spectra were registered for each peak of the corresponding chromatograms. Mass chromatograms, *i.e.* representations of mass spectrometry data as chromatograms (the  $x$ -axis representing time and the  $y$ -axis signal intensity), were registered using different scan ranges. The mass spectrometer was operated in both positive ( $\text{ESI}^+$ ) and negative ( $\text{ESI}^-$ ) ion modes. When solutions containing peptides and Ptr were analyzed, the signals corresponding to the intact molecular ion of Ptr as  $[\text{M} + \text{H}]^+$  and  $[\text{M} - \text{H}]^-$  species at  $m/z$  164 Da and 162 Da, respectively, were observed. However, in the case of the peptides, the resolution was much better in  $\text{ESI}^+$  than in  $\text{ESI}^-$  mode. Therefore all the results presented in this work correspond to mass spectrometry analysis carried out in  $\text{ESI}^+$  mode.

## 3. Results and Discussion

### 3.1. Degradation of $\alpha\text{-MSH}_{\text{Y2G}}$ Photo-induced by Pterin

The peptide  $\alpha\text{-MSH}_{\text{Y2G}}$ , derived from  $\alpha\text{-MSH}$  by mutation of the Tyr residue in position 2 to Gly, contains Trp as the residue most sensitive to oxidation reactions. When air-equilibrated aqueous solutions containing pterin (Ptr) were exposed to UV-A radiation (350 nm) in the presence of  $\alpha\text{-MSH}_{\text{Y2G}}$ , significant changes were

observed in the absorption spectra of the solutions (Fig. S1). Analysis by HPLC using an absorbance detector (HPLC-PDA, Experimental) showed that the chromatographic peak corresponding to  $\alpha\text{-MSH}_{\text{Y2G}}$  decreased with irradiation time (analysis at 280 nm, Fig. 2). However, the concentration of Ptr, determined by HPLC-PDA analysis at 340 nm, did not change within experimental error in agreement with the role of Ptr as a photosensitizer (Fig. 3). Concomitantly, new peaks were detected, revealing the formation of several photoproducts absorbing at wavelengths longer than 300 nm (Fig. 2). In addition,  $\text{H}_2\text{O}_2$  was generated and its concentration increased as a function of irradiation time (Fig. 3).

Trp is the only amino acid residue in  $\alpha\text{-MSH}_{\text{Y2G}}$  that absorbs at 295 nm and presents an intense emission band centered at 355 nm. We took advantage of these particular emission features and registered the emission spectra of the solutions at regular time intervals during irradiation. The decrease of the intensity of the emission band centered at 355 nm (excitation wavelength ( $\lambda_{\text{exc}}$ ) = 295 nm, Fig. S2) confirmed that the Trp residue in  $\alpha\text{-MSH}_{\text{Y2G}}$  was consumed upon Ptr irradiation. Moreover, chromatography coupled to a fluorescence detector (HPLC-FL,  $\lambda_{\text{exc}}$ : 295 nm,  $\lambda_{\text{em}}$ : 355 nm, Experimental) showed a main peak, with a retention time ( $t_r$ ) matching that of  $\alpha\text{-MSH}_{\text{Y2G}}$  in chromatograms obtained by HPLC-PDA analysis at 280 nm (Fig. 2). The intensity of this chromatographic peak also decreased during Ptr irradiation (Fig. 3).

Control experiments confirmed that, under otherwise identical conditions, no reaction occurs when solutions containing Ptr and  $\alpha\text{-MSH}_{\text{Y2G}}$

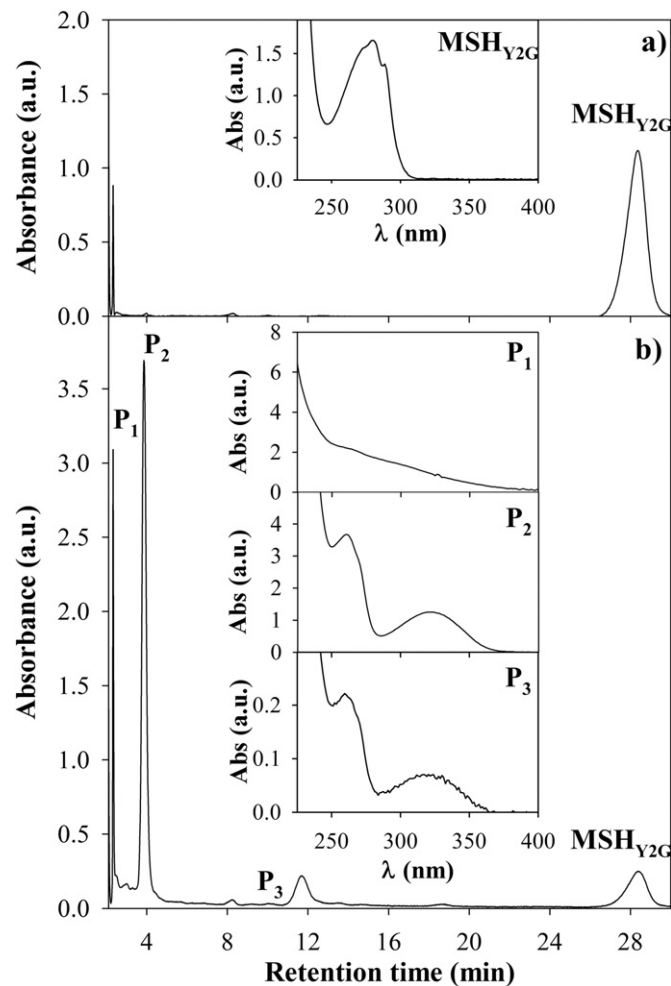
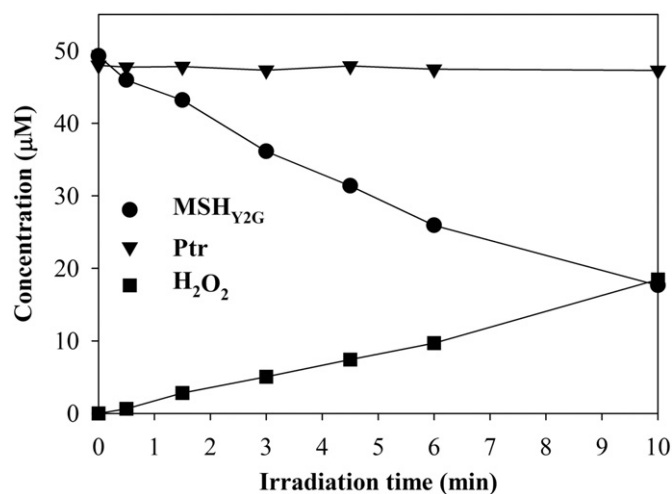


Fig. 2. Chromatograms obtained in HPLC-PDA analysis at 280 nm of  $\alpha\text{-MSH}_{\text{Y2G}}$ ; (a) before irradiation; (b) after 10 min of irradiation in the presence of Ptr. Insets: absorption spectra of the peptide and the photoproducts.  $[\text{Ptr}]_0 = 50 \mu\text{M}$ ,  $[\alpha\text{-MSH}_{\text{Y2G}}]_0 = 48 \mu\text{M}$ , pH = 5.5.



**Fig. 3.** Evolution of the Trp residue, Ptr and H<sub>2</sub>O<sub>2</sub> concentrations in air-equilibrated aqueous solutions under UV-A irradiation as a function of time. Concentrations of the Trp residue, Ptr and H<sub>2</sub>O<sub>2</sub> were determined by HPLC-FL ( $\lambda_{\text{exc}} = 295$  nm,  $\lambda_{\text{em}} = 355$  nm), by HPLC-PDA ( $\lambda_{\text{an}} = 340$  nm) and by an enzymatic method, respectively.  $[\alpha\text{-MSH}_{Y2G}]_0 = 48$   $\mu\text{M}$ ,  $[\text{Ptr}]_0 = 50$   $\mu\text{M}$ , pH = 5.5.

are kept in the dark or when  $\alpha\text{-MSH}_{Y2G}$  solutions are irradiated in the absence of Ptr.

### 3.2. Spectroscopic Characterization of $\alpha\text{-MSH}_{Y2G}$ Photoproducts

HPLC-PDA analysis showed that at least 3 major products were formed arbitrarily named P1, P2 and P3 (Fig. 2). Besides, several additional peaks with small areas were detected, all of them with  $t_r$  shorter than that of the intact peptide. Product P1 ( $t_r = 2.33$  min) presented an undefined spectrum and might be a mixture of several minor products. On the other hand, products P2 ( $t_r = 3.86$  min) and P3 ( $t_r = 11.63$  min) have spectral features similar to those reported for N-formylkynurenine (NFK). Excitation into the low-energy band of NFK results in a broad fluorescence band centered at 434 nm [21]. Fluorescence chromatograms obtained by HPLC-FL analysis ( $\lambda_{\text{exc}} = 325$  nm) revealed that products P2 and P3 emit at 432 nm and that their concentrations increased with irradiation time (Fig. 4). Under these experimental conditions, the intact peptide is not detected because it does not absorb at 325 nm (Fig. 1).

The product P2 was isolated from the HPLC runs (Experimental) at various irradiation times. The emission spectra upon excitation at 340 nm, recorded using a fluorometer (Experimental, Fig. 4), were identical to that reported in the literature for NFK [21], which has been proposed as a product of photosensitized reactions of Trp by several authors [22]. In contrast, P3 could not be isolated from HPLC runs at high enough concentration to register its emission spectrum, suggesting that P3 is formed at a lower rate than P2.

Hydroxy-tryptophan (HO-Trp) is another compound proposed as a product of the Ptr-photosensitized oxidation of free Trp [9] and has been identified in the skin of patients affected by vitiligo [23]. Further investigation of the minor peaks revealed that one of them ( $t_r = 3.71$  min) presented an absorption spectrum red shifted with respect to that of Trp (Fig. 5). In addition, this compound was isolated from HPLC runs and showed an emission spectrum, different from that recorder for P2, but similar to that of Trp. These spectroscopic properties are compatible with those reported for 5-hydroxy-tryptophan (5-HO-Trp) [24], suggesting that the detected photoproduct could be 5-HO-Trp residue or an isomer. It is worth mentioning that the concentration of this product, in contrast to the NFK residue, reached a maximum and then decreased, indicating that it was sensitive to Ptr-photosensitization.

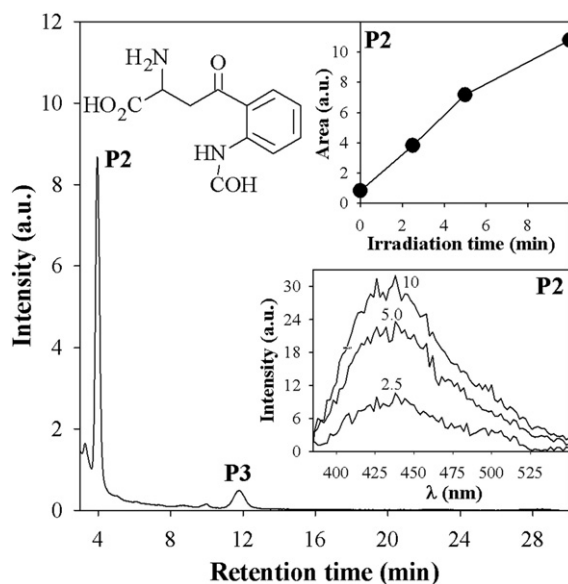


**Fig. 4.** Chromatogram obtained by HPLC-FL analysis ( $\lambda_{\text{exc}} = 325$  nm,  $\lambda_{\text{em}} = 435$  nm) of  $\alpha\text{-MSH}_{Y2G}$  after 10 min of irradiation in the presence of Ptr. Upper inset: time evolution of the area of the main peak ( $t_r = 3.9$  min). Lower inset: corrected fluorescence spectra ( $\lambda_{\text{exc}} = 340$  nm), registered on a fluorometer, of product P2 isolated from the HPLC equipment (the corresponding irradiation times (min) appear above each spectrum).  $[\text{Ptr}]_0 = 51$   $\mu\text{M}$ ,  $[\alpha\text{-MSH}_{Y2G}]_0 = 52$   $\mu\text{M}$ , pH = 5.5. Chemical structure of N-formylkynurenine.

### 3.3. Mass Spectrometry Analysis of $\alpha\text{-MSH}_{Y2G}$ Photoproducts

The photoproducts were also analyzed by UPLC coupled to mass spectrometry (UPLC-QToF-MS, Experimental). The mass chromatograms of irradiated solutions showed, besides the peaks corresponding to the reactants, two main peaks with  $t_r$  values of 7.2 and 9.7 min (Fig. 6a), arbitrarily called peaks B and A, respectively. The molecular formula of  $\alpha\text{-MSH}_{Y2G}$  is C<sub>70</sub>H<sub>104</sub>N<sub>21</sub>O<sub>18</sub>S and its molecular weight is 1559.7 Da. This value is an average of different weights due to the naturally

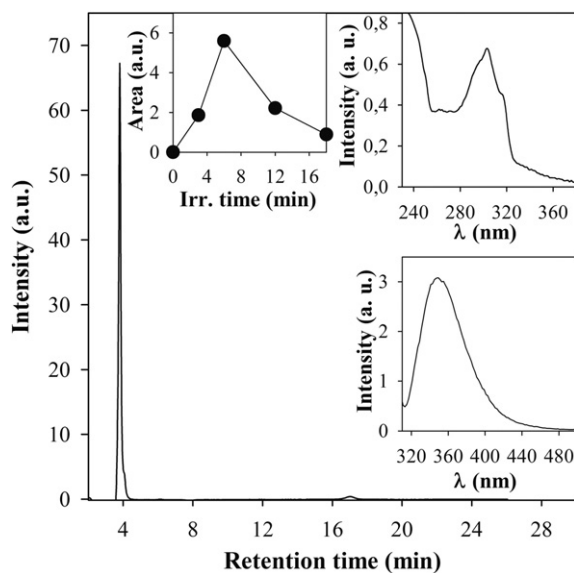


**Fig. 5.** Chromatogram obtained by HPLC-FL analysis ( $\lambda_{\text{exc}} = 315$  nm,  $\lambda_{\text{em}} = 330$  nm) of  $\alpha\text{-MSH}_{Y2G}$  after 6 min of irradiation of solutions containing Ptr as a photosensitizer. Upper left inset: time evolution of the area of the main peak ( $t_r = 4.0$  min). Upper right inset: absorption spectrum of the product. Lower inset: corrected fluorescence spectra ( $\lambda_{\text{exc}} = 295$  nm), registered on a fluorometer, of the product isolated from the HPLC.  $[\text{Ptr}]_0 = 100$   $\mu\text{M}$ ,  $[\alpha\text{-MSH}_{Y2G}]_0 = 80$   $\mu\text{M}$ , pH = 5.5.

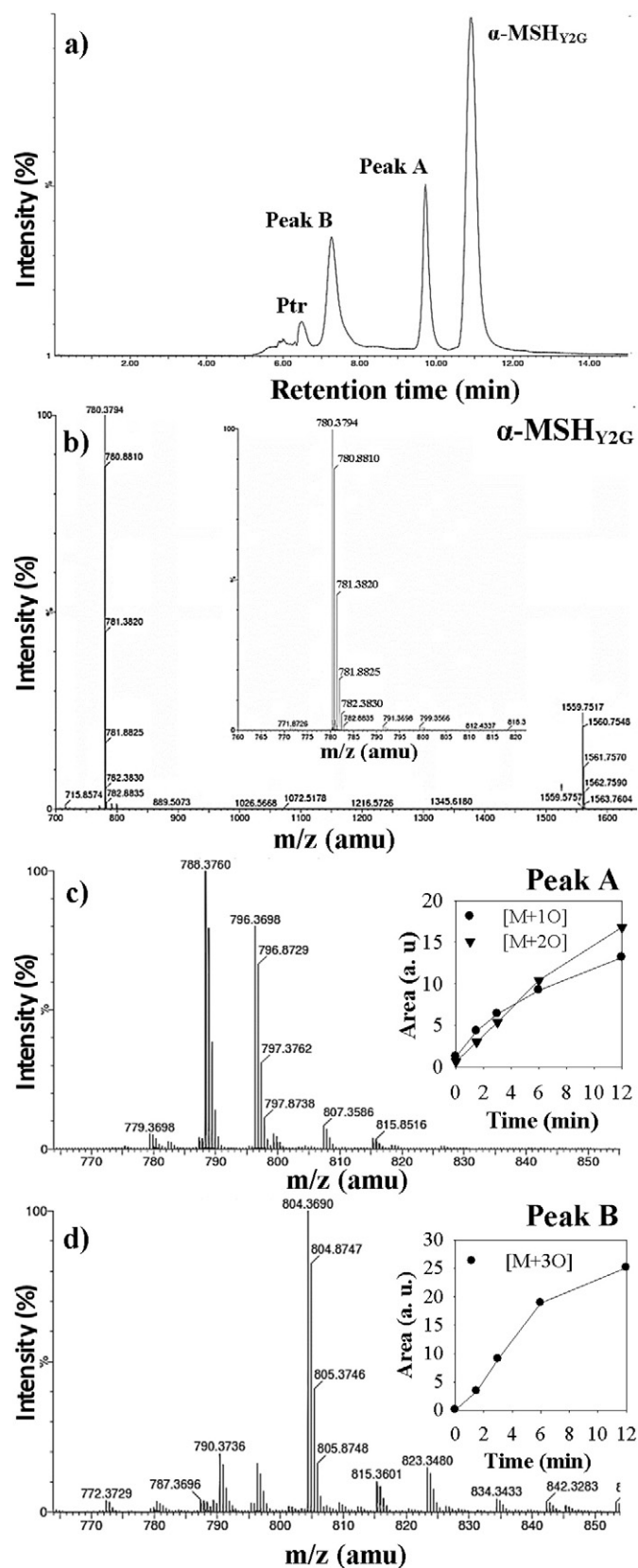


**Fig. 6.** UPLC-QToF-MS analysis of an  $\alpha$ -MSH<sub>Y2G</sub> solution (350  $\mu$ M) irradiated 12 min in the presence of Ptr (50  $\mu$ M). a) Mass chromatogram. b) Mass spectra of  $\alpha$ -MSH<sub>Y2G</sub>. Inset: Detail of the di-charged ions. c) and d) mass spectra of Peak A and Peak B, respectively; insets: time evolution of the area of the main peaks extracted from mass chromatograms registered for the corresponding specific masses ([M + O], [M + 2O], [M + 3O]).

occurring isotopes of carbon (natural abundance,  $^{12}\text{C}$ : 98.93%,  $^{13}\text{C}$ : 1.07%), although isotopes of nitrogen and oxygen also contribute. Therefore the registered mass spectrum of the chromatographic peak of  $\alpha$ -MSH<sub>Y2G</sub> consisted of groups of signals for the mono-charged ( $m/z \approx 1560$  Da), di-charged ( $m/z \approx 780$  Da) and tri-charged ions ( $m/z \approx 520$  Da). It should be noted that the group of signals corresponding to the di-charged ion is much more intense than that corresponding to the mono-charged ion (Fig. 6b).

Mass spectra of the products showed  $m/z$  values higher than those of the intact peptide and corresponding to oxygenated molecules. In particular, the mass spectrum of peak A revealed products with incorporation of one and two oxygen atoms ([M + O], [M + 2O]) (Fig. 6c). Peak B corresponded to a product that incorporated three oxygen atoms ([M + 3O]) (Fig. 6d). The mass chromatograms of irradiated solutions were registered for the specific ion masses of [M + O], [M + 2O] and [M + 3O] and the peaks were integrated. Data showed that the concentrations of the three oxygenated products increased as a function of irradiation time (Fig. 6b and c).

The detection of products with molecular weights [M + O] and [M + 2O] are in agreement with the findings obtained by HPLC-PDA and HPLC-FL analyses. Indeed oxidation of the Trp moiety to HO-Trp and NFK involves the incorporation of one and two oxygen atoms, respectively. It is worth mentioning that the time evolution of [M + O] concentration did not match with that of the product assigned to HO-Trp (*vide supra*). Although the experimental conditions of the corresponding experiments were different, very likely, HO-Trp is not the only product with mass [M + O].

The product with molecular weight [M + 3O] might correspond to a peptide with an NFK residue and an additional oxygen atom in another residue of the peptide sequence. This hypothesis is compatible with the fact that two products were detected with spectral properties matching those of NFK (Figs. 2 and 4). A potential target for Ptr-photosensitization, besides Trp, is the histidine (His) residue since the photo-induced oxidation of free His by Ptr has been recently demonstrated [11].

#### 3.4. Degradation of $\alpha$ -MSH<sub>W9G</sub> Photo-induced by Pterin

A series of experiments similar to that described in the sections above was performed using  $\alpha$ -MSH<sub>W9G</sub> as a substrate. This peptide has a Tyr residue and lacks Trp, therefore the chemical modifications undergone by the former can be analyzed. When air-equilibrated aqueous solutions containing Ptr were exposed to UV-A radiation in the presence of  $\alpha$ -MSH<sub>W9G</sub>, the spectral changes were almost negligible. Nevertheless, HPLC-PDA analysis showed that  $\alpha$ -MSH<sub>W9G</sub> was consumed upon irradiation and that several photoproducts were formed (Fig. 7).

As the fluorescence at 300 nm of  $\alpha$ -MSH<sub>W9G</sub> upon excitation at 275 nm can be attributed to Tyr residues [10,24], the effect of the Ptr photosensitized process on this residue could be also investigated by HPLC-FL. Fluorescence chromatograms ( $\lambda_{\text{exc}} = 275$  nm,  $\lambda_{\text{em}} = 300$  nm) showed a main peak, with a  $t_r$  value matching that of the peak of the peptide in HPLC-PDA chromatograms at 275 nm (Fig. 7). Results confirmed that the Tyr residue was consumed during irradiation of Ptr solutions containing  $\alpha$ -MSH<sub>W9G</sub>, whereas the concentration of the photosensitizer did not change (Fig. 8). As in the case of  $\alpha$ -MSH<sub>Y2G</sub>, H<sub>2</sub>O<sub>2</sub> was generated and its concentration increased as a function of irradiation time (Fig. 8). It is worth mentioning that comparison of Figs. 3 and 8 reveals that for the same experimental conditions the consumption of Trp in  $\alpha$ -MSH<sub>Y2G</sub> is slightly faster than that of Tyr in  $\alpha$ -MSH<sub>W9G</sub>. But the opposite behavior was observed when both amino acid residues were in the same peptide [17]. These facts indicate that small differences in the composition of the peptides change to some extent the relative reactivity of both amino acid residues.

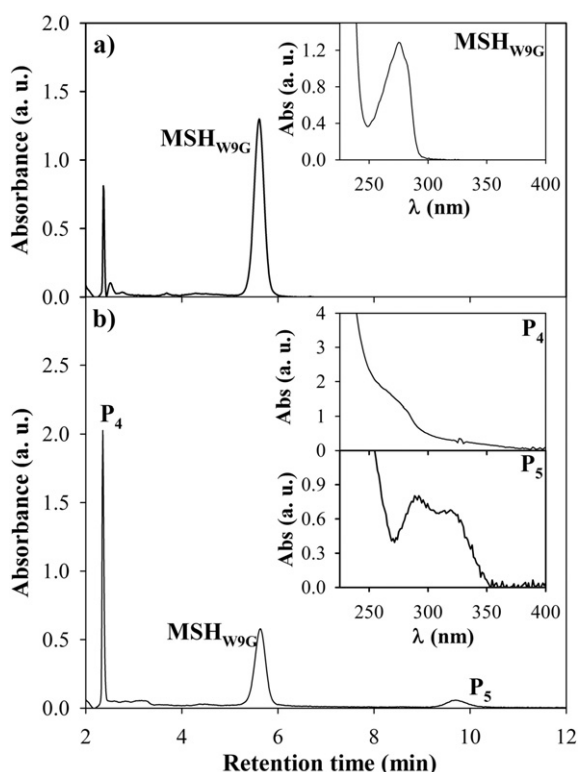


**Fig. 7.** Chromatograms obtained by HPLC-PDA analysis of  $\alpha$ -MSH<sub>W9G</sub> at 275 nm; (a) before irradiation; (b) after 10 min of irradiation of solutions containing Ptr as a photosensitizer. Insets: absorption spectra of the peptide and of the photoproducts. [Ptr]<sub>0</sub> = 49  $\mu$ M, [ $\alpha$ -MSH<sub>W9G</sub>]<sub>0</sub> = 48  $\mu$ M, pH = 5.5.

### 3.5. Spectroscopic Characterization of $\alpha$ -MSH<sub>W9G</sub> Photoproducts

HPLC-PDA analysis showed that, at least two major products were formed, arbitrarily called P4 and P5 (Fig. 7). Product P5 has  $t_r$  longer than the intact peptide. HPLC-FL chromatograms showed that P5 emits at 405 upon excitation at 310 nm (Fig. 9). The product P5 could be isolated from the HPLC runs and its emission spectrum is similar to that reported for the dimer *o,o'*-dityrosine (Tyr<sub>2</sub>) [25] (broad fluorescence band centered at 410–420 nm by excitation into the low-energy band) (Fig. 9). It is known since the 1960s that the one-electron

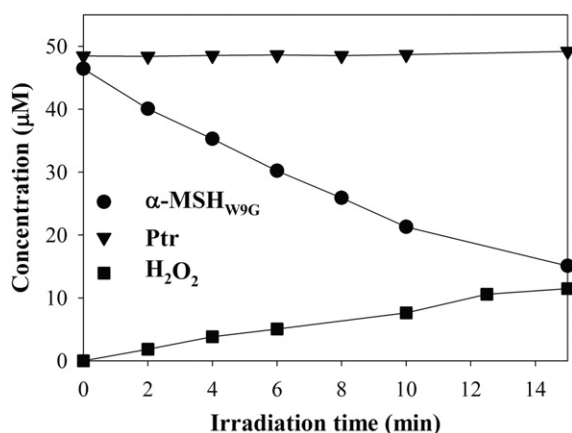


**Fig. 8.** Evolution of the Tyr residue, Ptr and H<sub>2</sub>O<sub>2</sub> concentrations in air-equilibrated aqueous solutions under UV-A irradiation as a function of irradiation time. Concentrations of the Tyr residue, Ptr and H<sub>2</sub>O<sub>2</sub> were determined by HPLC-FL ( $\lambda_{exc}$  = 275 nm,  $\lambda_{em}$  = 300 nm), by HPLC-UV ( $\lambda_{an}$  = 340 nm) and by an enzymatic method, respectively. [ $\alpha$ -MSH<sub>W9G</sub>]<sub>0</sub> = 48  $\mu$ M, [Ptr]<sub>0</sub> = 49  $\mu$ M, pH = 5.5.

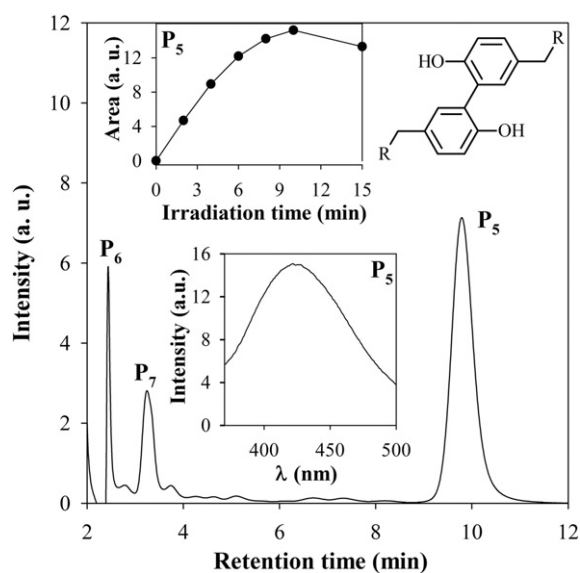


**Fig. 9.** Chromatogram obtained by HPLC-FL analysis ( $\lambda_{exc}$  = 310 nm,  $\lambda_{em}$  = 405 nm) of  $\alpha$ -MSH<sub>W9G</sub> after 10 min of irradiation of solutions containing Ptr as a photosensitizer. Upper inset: time evolution of the area of the main peak ( $t_r$  = 9.8 min). Lower inset: corrected fluorescence spectrum ( $\lambda_{exc}$  = 295 nm), registered on a fluorometer, of the main photoproduct isolated from the HPLC equipment (irradiation time: 8 min). [Ptr]<sub>0</sub> = 50  $\mu$ M, [ $\alpha$ -MSH<sub>W9G</sub>]<sub>0</sub> = 48  $\mu$ M, pH = 5.5. Chemical structure of the main form of Tyr<sub>2</sub>, the dimer *o,o'*-dityrosine.

oxidation of Tyr generates the long-lived tyrosyl radical (Tyr(-H)<sup>•</sup>) and that coupling of two Tyr(-H)<sup>•</sup> radicals yields the dimer *o,o'*-dityrosine as the main product [26,27]. It is worth mentioning that in the experiment shown in Fig. 9, the Tyr<sub>2</sub> fluorescence-like emission increased up to a maximum value and then decreased, indicating that dimers are not photostable.

The radical in Tyr(-H)<sup>•</sup> being delocalized on the aromatic ring, dimerization can lead to other isomers besides *o,o'*-dityrosine [28]. In the case of  $\alpha$ -MSH<sub>W9G</sub>, we also detected by HPLC-FL analysis two additional products (P6 and P7) with emission features compatible with the Tyr<sub>2</sub> structure (Fig. 9), both of them corresponded to very small peaks in the HPLC-PDA chromatograms (Fig. 7).

### 3.6. Mass Spectrometry Analysis of $\alpha$ -MSH<sub>W9G</sub> Photoproducts

The molecular formula of  $\alpha$ -MSH<sub>W9G</sub> is C<sub>68</sub>H<sub>103</sub>N<sub>20</sub>O<sub>19</sub>S and its molecular weight is 1536.6 Da. As in the case of  $\alpha$ -MSH<sub>Y2C</sub> (*vide supra*), this value is an average of different weights due to the naturally occurring isotopes. Therefore the mass spectrum of  $\alpha$ -MSH<sub>W9G</sub> recorded in UPLC-QToF-MS analysis consisted of groups of signals for the mono-charged ( $m/z$   $\approx$  1537.7 Da), di-charged ( $m/z$   $\approx$  769.3 Da) and tri-charged ions ( $m/z$   $\approx$  513.2 Da). The group of signals corresponding to the di-charged ion was again much more intense than that corresponding to the mono-charged ion (Fig. 10).

The mass chromatograms of irradiated solutions showed, besides the peaks corresponding to the reactants, many peaks whose areas increased with irradiation time (Fig. 10a). Two of the peaks (C and D, Fig. 10a) presented mass spectra with groups of signals at  $m/z$   $\approx$  1536.7 Da, 1024.8 Da and 768.8 Da (Fig. 10b). Comparison with the group of signals of the di-charged ion of the intact peptide clearly indicates that the signals around  $m/z$   $\approx$  768.8 Da correspond to tetra-charged ions of a molecule with molecular weight [2 $\alpha$ -MSH<sub>W9G</sub>-2H] (Fig. 10c and d). Signals at  $m/z$   $\approx$  1536.7 Da and 1024.8 Da of the mass spectra of peaks C and D (Fig. 10b) correspond to di and tri-charged ions, respectively. This result confirmed the formation of a Tyr<sub>2</sub> moiety, already suggested by the results of HPLC-PDA and HPLC-FL (*vide supra*). The fact that two products showed the same mass spectrum is again in agreement with the HPLC-FL analysis and can be

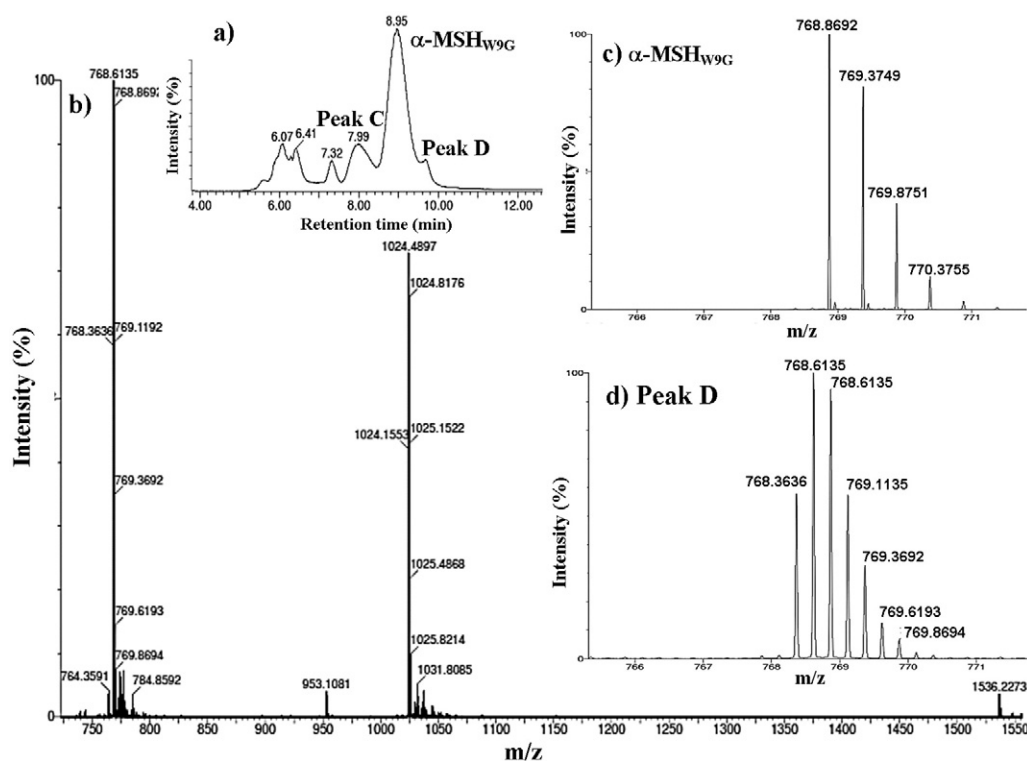


**Fig. 10.** UPLC-QToF-MS analysis of an  $\alpha$ -MSH<sub>W9G</sub> solution (320  $\mu$ M) irradiated during 12 min in the presence of Ptr (50  $\mu$ M). a) Mass chromatogram. b) Mass spectra of  $\alpha$ -MSH<sub>W9G</sub>. c) Mass spectra of  $\alpha$ -MSH<sub>W9G</sub>: detail of the di-charged ions. d) Mass spectra of Peak D: detail of the tetra-charged ions.

attributed to different isomers of the Tyr<sub>2</sub> structure. In control analyses of the solutions before irradiation, no dimeric-type products could be detected.

The analysis of mass spectra of the other peaks revealed, at least, two photoproducts that incorporated one oxygen atom ( $[M + O]$ ), but only one that bore two oxygen atoms ( $[M + 2O]$ ). This fact suggests that there are two main different positions for the incorporation of oxygen into the peptide moiety. In addition, dimeric products with incorporation of one, two and three oxygen atoms ( $[2M - 2H + O]$ ,  $[2M - 2H + 2O]$ ,  $[2M - 2H + 3O]$ ,  $[2M - 2H + 4O]$ ) were also detected. The mass chromatograms of irradiated solutions registered for the specific ion masses corresponding to the oxygenated monomeric and dimeric products revealed that all of them increased their concentrations as a function of irradiation time. These results indicate that upon irradiation of Ptr,  $\alpha$ -MSH<sub>W9G</sub> undergoes two simultaneous processes: dimerization and incorporation of oxygen.

### 3.7. Mechanistic Analysis

We checked if the mechanism proposed for the photosensitized oxidation of  $\alpha$ -MSH (ref. 17, Introduction) was also valid for the mutated peptides investigated in this work. Steady-state photolyses were carried out under different experimental conditions and the evolution of the concentrations of substrates and their main photoproducts were analyzed as a function of the irradiation time by HPLC-FL. In particular, for  $\alpha$ -MSH<sub>V2G</sub> the consumption of Trp residues ( $\lambda_{exc} = 295$  nm,  $\lambda_{em} = 355$  nm) and the production of NFK residues were evaluated ( $\lambda_{exc} = 325$  nm,  $\lambda_{em} = 434$  nm). For  $\alpha$ -MSH<sub>W9G</sub>, the consumption of Tyr residues ( $\lambda_{exc} = 275$  nm,  $\lambda_{em} = 300$  nm) and the production of the Tyr<sub>2</sub> moiety ( $\lambda_{exc} = 310$  nm,  $\lambda_{em} = 400$  nm) were investigated.

For both peptides no photochemical reaction was observed under anaerobic conditions, thus indicating that O<sub>2</sub> is needed for the photosensitization, which is consistent with the behavior reported for  $\alpha$ -MSH [17] and free Trp [9] and Tyr [10]. In another set of experiments, photolyses were carried out in O<sub>2</sub>-saturated solutions. Results revealed

that the reactions were faster in air-equilibrated than in O<sub>2</sub>-saturated solutions (Fig. 11).

It has been previously demonstrated that iodide (I<sup>-</sup>) at micromolar concentrations is an efficient and selective quencher of triplet excited states of pterins [29,30]. For both peptides, the rate of consumption was slower in the presence than in the absence of I<sup>-</sup> (Fig. 11), in agreement with a photosensitized reaction initiated by the triplet excited state of Ptr.

Since Ptr is a <sup>1</sup>O<sub>2</sub> photosensitizer [16], we investigated the contribution of this species by performing comparative experiments using H<sub>2</sub>O and D<sub>2</sub>O as solvents. Given that the <sup>1</sup>O<sub>2</sub> lifetime ( $\tau_{\Delta}$ ) in D<sub>2</sub>O is longer than that in H<sub>2</sub>O by a factor of approximately 15 [31,32], the Ptr-photosensitized degradation of the peptides should be much faster in D<sub>2</sub>O if <sup>1</sup>O<sub>2</sub> contributed significantly to the process. Air-equilibrated solutions containing a given peptide and Ptr (50  $\mu$ M) in H<sub>2</sub>O and D<sub>2</sub>O at pH/pD 5.5 were irradiated under otherwise identical conditions. The time evolution of the concentration of Trp and NFK residues for  $\alpha$ -MSH<sub>V2G</sub> and of Tyr and Tyr<sub>2</sub> residues for  $\alpha$ -MSH<sub>W9G</sub> were determined by HPLC-FL (Fig. 12).

In the case of  $\alpha$ -MSH<sub>V2G</sub>, results showed that the rate of the degradation of the peptide was hardly faster in D<sub>2</sub>O than in H<sub>2</sub>O. Nevertheless, it is worth mentioning that the production of NFK residue was significantly higher in D<sub>2</sub>O than in H<sub>2</sub>O, which could be expected since NFK is a typical product of the oxidation of free Trp by <sup>1</sup>O<sub>2</sub> [22]. However, the increase in the rate of oxidation of the Trp residue to NFK was not as large as could have been expected from the differences in <sup>1</sup>O<sub>2</sub> lifetimes in the two solvents. This fact suggests that NFK might be also formed *via* another mechanism (type I). In addition, although the increase in the production of NFK was significant in D<sub>2</sub>O compared to H<sub>2</sub>O, the increase in the rate of peptide consumption was not (Fig. 12a). This result suggests that the oxidation of the Trp residue to yield NFK is not the main pathway for the consumption of the reactant.

In the case of  $\alpha$ -MSH<sub>W9G</sub>, the rate of the degradation of the peptide was slightly faster in D<sub>2</sub>O than in H<sub>2</sub>O, but again not to the extent expected from the differences in <sup>1</sup>O<sub>2</sub> lifetimes in the two solvents. The

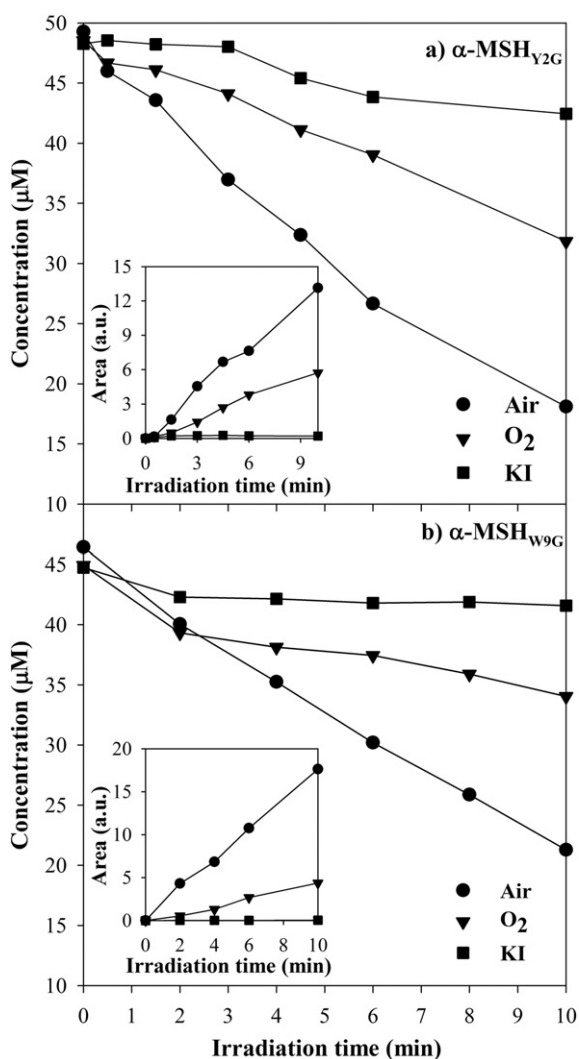


**Fig. 11.** HPLC-FL analysis of a)  $\alpha$ -MSH<sub>Y2G</sub> and b)  $\alpha$ -MSH<sub>W9G</sub> in air-equilibrated aqueous solutions irradiated in the presence of Ptr in the absence of KI (●) and in the presence of KI (400  $\mu$ M) (■), and in O<sub>2</sub> equilibrated solutions (▼). a) Concentration of the Trp residue ( $\lambda_{\text{exc}} = 295$  nm,  $\lambda_{\text{em}} = 355$  nm) as a function of irradiation time. Inset: time evolution of the area of the peak assigned to NFK ( $\lambda_{\text{exc}} = 325$  nm,  $\lambda_{\text{em}} = 434$  nm). b) Concentration of the Tyr residue ( $\lambda_{\text{exc}} = 275$  nm,  $\lambda_{\text{em}} = 300$  nm) as a function of irradiation time. Inset: time evolution of the area of the peak assigned to the Tyr<sub>2</sub> structure ( $\lambda_{\text{exc}} = 310$  nm,  $\lambda_{\text{em}} = 400$  nm). [ $\alpha$ -MSH<sub>Y2G</sub>]<sub>0</sub> = 45  $\mu$ M, [ $\alpha$ -MSH<sub>W9G</sub>]<sub>0</sub> = 46  $\mu$ M, [Ptr]<sub>0</sub> = 48  $\mu$ M, pH = 5.5.

rate of production of the Tyr<sub>2</sub> moiety was identical, within experimental error, in both solvents (Fig. 12). This is in agreement with the reported result that Tyr<sub>2</sub> structures are not formed by oxidation with <sup>1</sup>O<sub>2</sub> [33,34].

Therefore, if the contribution of <sup>1</sup>O<sub>2</sub> to the oxidation of the peptides may be discarded or is minor, a degradation mechanism initiated by an electron transfer from the amino acid to the triplet excited state of Ptr (<sup>3</sup>Ptr\*) should be dominant, as in the case of  $\alpha$ -MSH [17]. Hence, two reactions compete for the bimolecular quenching of <sup>3</sup>Ptr\* in the system: i) energy transfer to dissolved O<sub>2</sub> producing <sup>1</sup>O<sub>2</sub> and regenerating Ptr (Reaction (5)); ii) electron transfer to yield the Ptr radical anion (Ptr<sup>•-</sup>) and the peptide radical cation (P<sup>•+</sup>), the dominant initiating step leading to the degradation of the peptide (Reaction (6)).



Since <sup>1</sup>O<sub>2</sub> plays a minor (or no) role in the oxidation of the peptide, an increase in the O<sub>2</sub> concentration, and therefore a more efficient

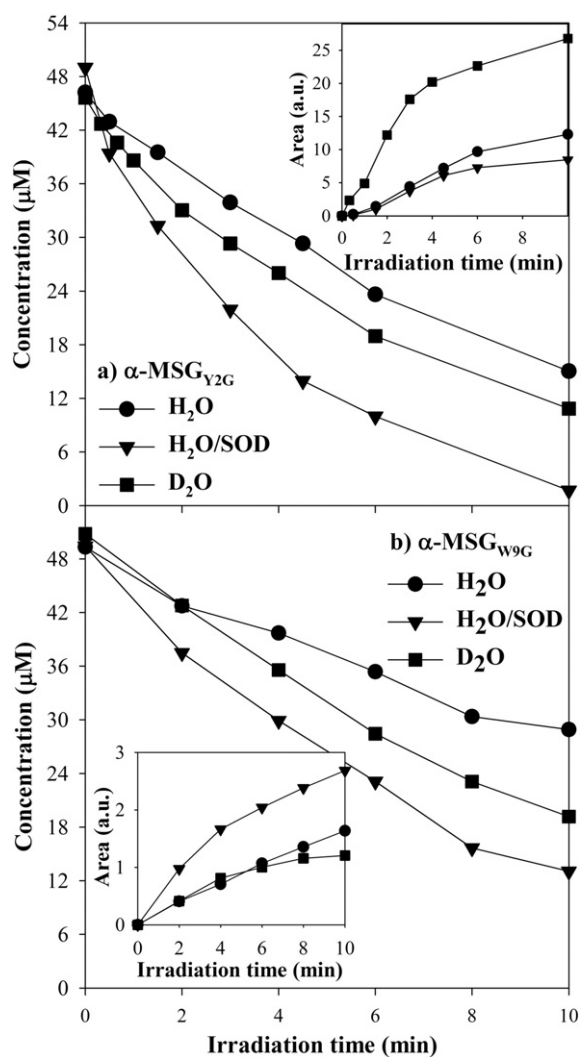


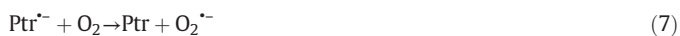
**Fig. 12.** HPLC-FL analysis of a)  $\alpha$ -MSH<sub>Y2G</sub> and b)  $\alpha$ -MSH<sub>W9G</sub> irradiated in the presence of Ptr in air-equilibrated H<sub>2</sub>O solutions in the absence of SOD (●) and in the presence of SOD (50 U/mL) (▼), and in D<sub>2</sub>O solutions (■). a) Concentration of the Trp residue ( $\lambda_{\text{exc}} = 295$  nm,  $\lambda_{\text{em}} = 355$  nm) as a function of irradiation time. Inset: time evolution of the area of the peak assigned to NFK ( $\lambda_{\text{exc}} = 325$  nm,  $\lambda_{\text{em}} = 434$  nm). b) Concentration of the Tyr residue ( $\lambda_{\text{exc}} = 275$  nm,  $\lambda_{\text{em}} = 300$  nm) as a function of irradiation time. Inset: time evolution of the area of the peak assigned to Tyr<sub>2</sub> ( $\lambda_{\text{exc}} = 310$  nm,  $\lambda_{\text{em}} = 400$  nm). [ $\alpha$ -MSH<sub>Y2G</sub>]<sub>0</sub> = 80  $\mu$ M, [ $\alpha$ -MSH<sub>W9G</sub>]<sub>0</sub> = 80  $\mu$ M, [Ptr]<sub>0</sub> = 48  $\mu$ M, pH = 5.5.

quenching of <sup>3</sup>Ptr\* by O<sub>2</sub> (Reaction (5)), should lead to a slower consumption of the peptides. Experiments performed in O<sub>2</sub>-saturated and in air-equilibrated solutions confirmed this effect (Fig. 11).

Following the electron transfer reaction (Reaction (6)), the organic radical anion Ptr<sup>•-</sup> will be readily quenched by ground state O<sub>2</sub> to produce the superoxide anion (O<sub>2</sub><sup>•-</sup>) [35,36], and regenerate Ptr (Reaction (7)). The spontaneous disproportionation of O<sub>2</sub><sup>•-</sup> in aqueous solution leads to the formation of H<sub>2</sub>O<sub>2</sub> as detected (*vide supra*) [37] (Reaction (8)). The participation of O<sub>2</sub><sup>•-</sup> in the mechanism was confirmed by performing experiments in the presence of superoxide dismutase (SOD), an enzyme that catalyzes the conversion of O<sub>2</sub><sup>•-</sup> into H<sub>2</sub>O<sub>2</sub> and O<sub>2</sub> [38]. A significant increase in the rate of consumption of the Trp and Tyr residues was observed when SOD was present in the solution (Fig. 12). This result indicates that i) O<sub>2</sub><sup>•-</sup> is involved in the photosensitized process and provides further evidence for the existence of an electron transfer reaction, ii) trapping of O<sub>2</sub><sup>•-</sup> by SOD competes with a reaction that prevents the oxidation of the amino acid residues. In fact, the peptide radical cations (P<sup>•+</sup>) or their deprotonated forms (neutral radicals P(-H)<sup>•</sup>, Reaction (9)) can react with O<sub>2</sub><sup>•-</sup> to regenerate the peptide (Reactions (10) and (10')). As a



consequence, faster elimination of  $O_2^{\cdot-}$  by SOD leads to the enhancement of the photosensitized oxidation of the amino acids observed experimentally (Fig. 12).



The reactivity of  $P^{*+}$  depends on the most reactive amino acid residue in the peptide sequence (Trp or Tyr). The radical cation is mainly located on the Trp residue in  $\alpha$ -MSH<sub>Y2G</sub> ( $Trp^{*+}$ ) and on the Tyr residue in  $\alpha$ -MSH<sub>W9G</sub> ( $Tyr^{*+}$ ). These radical cations and the corresponding neutral radicals ( $P^{*+}/P(-H)^{\cdot}$ ) participate in different reactions to yield products. For both peptides investigated, oxidation with incorporation of one or more oxygen atoms was observed (Reactions (11), (11'), (11'') and (12)), whereas dimerization only occurred in the case of  $\alpha$ -MSH<sub>W9G</sub> (Reaction (13)).



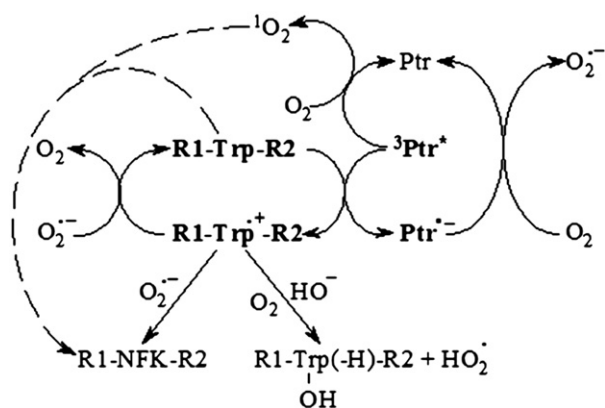
For both peptides, the formation of the oxidized products with the incorporation of 1 oxygen atom may be explained by the addition of the hydroxide anion (hydration) to the radical cation (Reaction (11)). This reaction yield a hydroxylated radical that traps  $O_2$  yielding to the corresponding peroxy radical (Reaction (11')). The latter may release  $HO_2^{\cdot}$  to form a stable oxidized product (Reaction (11'')). The charges on  $Trp^{*+}$  and  $Tyr^{*+}$  are delocalized on different sites of the molecules and several hydroxylated products (on the aromatic or pyrrole rings for Trp and on the benzene ring for Tyr) may be formed [9]. Two hydroxylated products (OH-Tyr-) may be formed in the first step in the case of the Tyr residue ( $\alpha$ -MSH<sub>W9G</sub>), as observed experimentally. Hydroxylation of the Trp residue of  $\alpha$ -MSH<sub>Y2G</sub> may yield up to five isomers.

It should be noted that, in the case of  $\alpha$ -MSH<sub>Y2G</sub>, NFK could be the product of the reaction between  $Trp^{*+}$  and superoxide (Reaction (12)) although it is in part formed by a  $^1O_2$ -mediated oxidation (Reaction (14)). The product bearing three oxygen atoms might be a peptide containing the Trp residue oxidized to NFK and another oxidized residue (e.g. histidine).



#### 4. Conclusions

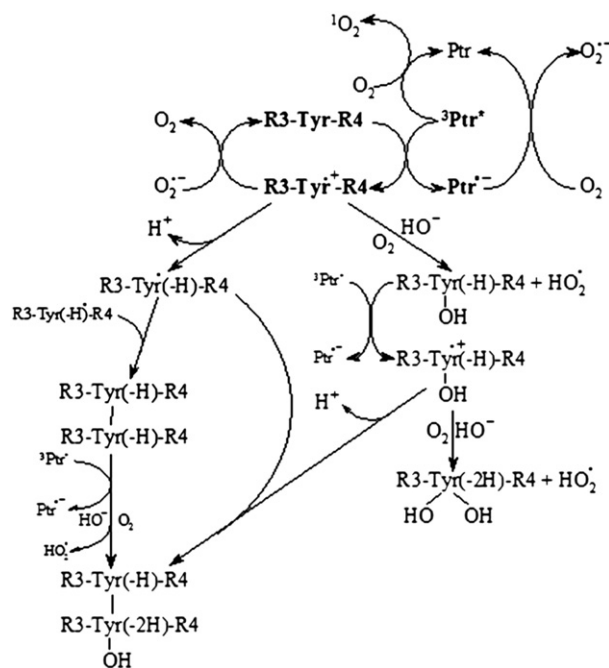
Unconjugated oxidized pterins accumulate in the skin of patients suffering from vitiligo, a chronic depigmentation disorder, and are able to induce a photosensitized damage to the peptide  $\alpha$ -melanocyte-stimulating hormone ( $\alpha$ -MSH). In a previous work, we have shown that, among the amino acid residues in the  $\alpha$ -MSH sequence, tryptophan (Trp) and tyrosine (Tyr) were most sensitive to oxidation. However, the analysis was complex because several consecutive and parallel reactions took place in the system. In the present work, we



**Scheme 2.** Main reaction pathways proposed for the Ptr-photosensitized degradation of the Trp residue in the  $\alpha$ -MSH<sub>Y2G</sub> peptide (R1-Trp-R2).

could get further insight into the mechanisms involved in the photosensitized degradation of  $\alpha$ -MSH by investigating the specific reactivity of two peptides ( $\alpha$ -MSH<sub>W9G</sub> or  $\alpha$ -MSH<sub>Y2G</sub>). In these peptides, the amino acid sequence of  $\alpha$ -MSH was mutated, the Trp or the Tyr residue being replaced by a glycine (Gly) residue, respectively. The parent compound of oxidized pterins (Ptr) was used as a model photosensitizer in aqueous solution at pH 5.5 and was exposed to UV-A radiation, a wavelength range where the peptides do not absorb.

The mechanistic analysis confirmed that, in both cases ( $\alpha$ -MSH<sub>W9G</sub> and  $\alpha$ -MSH<sub>Y2G</sub>), the role of singlet oxygen ( $^1O_2$ ) produced by energy transfer from  $^3Ptr^*$  to dissolved  $O_2$  (type II mechanism) was negligible or minor. The dominant reaction pathways are initiated by an electron transfer from the peptide to the Ptr triplet excited state ( $^3Ptr^*$ ) (Reaction (6), type I mechanism). The subsequent electron transfer from the Ptr radical anion ( $Ptr^{\cdot-}$ ) to  $O_2$  regenerates Ptr and forms  $O_2^{\cdot-}$ , which in turn disproportionates to  $H_2O_2$ . The resulting radical cations, mainly located on the Trp residue in  $\alpha$ -MSH<sub>Y2G</sub> ( $Trp^{*+}$ ) and on the Tyr residue in  $\alpha$ -MSH<sub>W9G</sub> ( $Tyr^{*+}$ ), undergo further reactions responsible for the degradation of the peptide (Schemes 2 and 3).



**Scheme 3.** Main reaction pathways proposed for the Ptr-photosensitized degradation of the Tyr residue in the  $\alpha$ -MSH<sub>W9G</sub> peptide (R3-Tyr-R4).

In the case of  $\alpha$ -MSH<sub>Y2G</sub>, the photosensitized process led to the formation of oxidized products. Two photoproducts involving the Trp residue were identified: hydroxy-tryptophan (HO-Trp(—H)) and N-formylkynurenine (NFK) that correspond to the incorporation of one and two oxygen atoms, respectively (Scheme 2). In a minor pathway, the latter compound can be also generated by oxidation of the Trp residue by singlet oxygen (<sup>1</sup>O<sub>2</sub>). The incorporation of up to three oxygen atoms suggests that the oxidation may take place in another amino acid residue, such as histidine, which is able to be photooxidized by Ptr in its free form. Further studies are required to evaluate the pterin-photosensitized oxidation of this amino acid in a peptide environment.

In the case of  $\alpha$ -MSH<sub>W9G</sub> two processes occurred: oxidation and dimerization (Scheme 3). The latter process was evidenced by the formation of several compounds with molecular weights corresponding to two molecules of the peptide. In these compounds the typical spectroscopic features of dimers of Tyr (Tyr<sub>2</sub>) were registered and dimerization was not detected for  $\alpha$ -MSH<sub>Y2G</sub> that lacks Tyr. Therefore, in the sequence of  $\alpha$ -MSH, the only amino acid residue responsible for peptide crosslinking is Tyr. The oxidation took place in both monomer and dimers, revealing that dimerization and oxidation are independent and simultaneous processes.

Supplementary data to this article can be found online at <http://dx.doi.org/10.1016/j.jphotobiol.2016.09.024>.

## Acknowledgements

The present work was partially supported by Consejo Nacional de Investigaciones Científicas y Técnicas (CONICET-Grant PIP 112-200901-00425), Agencia de Promoción Científica y Tecnológica (ANPCyT-Grant PICT-2012-0508), Universidad Nacional de La Plata (UNLP-Grant X712). The authors thank the Centre National de la Recherche Scientifique (CNRS) and CONICET for supporting their collaboration through a Programme de Coopération Scientifique (CONICET-CNRS/PICS N°05920). C.C. thanks CONICET for her doctoral research fellowship. M.V. and A.H.T. are research members of CONICET. P.V and E.O are research members of CNRS. The authors also thank Nathalie Martins-Froment of the Service Commun de Spectrométrie de Masse (FR2599), Université de Toulouse III (Paul Sabatier) for their valuable help with the mass spectrometry measurements.

## References

- [1] Y. Matsumura, H.N. Ananthaswamy, Toxic effects of ultraviolet radiation on the skin, *Toxicol. Appl. Pharmacol.* 195 (2004) 298–308.
- [2] J. Cadet, T. Douki, Oxidatively generated damage to DNA by UVA radiation in cells and human skin, *J. Invest. Dermatol.* 131 (2011) 1005–1007.
- [3] S.E. Braslavsky, Glossary of terms used in photochemistry 3rd edition: (IUPAC recommendations 2006), *Pure Appl. Chem.* 79 (2007) 293–465.
- [4] M.J. Davies, Singlet oxygen-mediated damage to proteins and its consequences, *Biochem. Biophys. Res. Commun.* 305 (2003) 761–770.
- [5] J. Cadet, E. Sage, T. Douki, Ultraviolet radiation-mediated damage to cellular DNA, *Mutat. Res. Fundam. Mol. Mech. Mutagen.* 571 (2005) 3–17.
- [6] D.I. Pattison, A.S. Rahmanto, M.J. Davies, Photo-oxidation of proteins, *Photochem. Photobiol. Sci.* 11 (2012) 38–53.
- [7] A.H. Thomas, C. Lorente, K. Roitman, M.M. Morales, M.L. Dántola, Photosensitization of bovine serum albumin by pterin: a mechanistic study, *J. Photochem. Photobiol. B Biol.* 120 (2013) 52–58.
- [8] A.H. Thomas, B.N. Zurbano, C. Lorente, J. Santos, E.A. Roman, M. Laura Dántola, Chemical changes in bovine serum albumin photoinduced by pterin, *J. Photochem. Photobiol. B Biol.* 141 (2014) 262–268.
- [9] A.H. Thomas, M.P. Serrano, V. Rahal, P. Vicendo, C. Claparols, E. Oliveros, C. Lorente, Tryptophan oxidation photosensitized by pterin, *Free Radic. Biol. Med.* 63 (2013) 467–475.
- [10] C. Castaño, M.L. Dántola, E. Oliveros, A.H. Thomas, C. Lorente, Oxidation of tyrosine photoinduced by pterin in aqueous solution, *Photochem. Photobiol.* 89 (2013) 1448–1455.
- [11] C. Castaño, E. Oliveros, A.H. Thomas, C. Lorente, Histidine oxidation photosensitized by pterin: PH dependent mechanism, *J. Photochem. Photobiol. B Biol.* 153 (2015) 483–489.
- [12] I. Ziegler, Production of pteridines during hematopoiesis and T-lymphocyte proliferation: potential participation in the control of cytokine signal transmission, *Med. Res. Rev.* 10 (1990) 95–114.
- [13] C.A. Nichol, G.K. Smith, D.S. Duch, Biosynthesis and metabolism of tetrahydrobiopterin and molybdopterin, *Annu. Rev. Biochem.* 54 (1985) 729–764.
- [14] S.J. Glassman, Vitiligo, reactive oxygen species and T-cells, *Clin. Sci.* 120 (2010) 99–120.
- [15] K.U. Schallreuter, J. Moore, J.M. Wood, W.D. Beazley, E.M. Peters, L.K. Marles, S.C. Behrens-Williams, R. Dummer, N. Blau, B. Thöny, Epidermal H<sub>2</sub>O<sub>2</sub> accumulation alters tetrahydrobiopterin (6BH<sub>4</sub>) recycling in vitiligo: identification of a general mechanism in regulation of all 6BH<sub>4</sub>-dependent processes? *J. Invest. Dermatol.* 116 (2001) 167–174.
- [16] C. Lorente, A.H. Thomas, Photophysics and photochemistry of pterins in aqueous solution, *Acc. Chem. Res.* 39 (2006) 395–402.
- [17] C. Castaño, C. Lorente, N. Martins-Froment, E. Oliveros, A.H. Thomas, Degradation of  $\alpha$ -melanocyte-stimulating hormone photosensitized by pterin, *Org. Biomol. Chem.* 12 (2014) 3877–3886.
- [18] C.C. Allain, L.S. Poon, C.S.G. Chan, W. Richmond, P.C. Fu, Enzymatic determination of total serum cholesterol, *Clin. Chem.* 20 (1974) 470–475.
- [19] H.M. Flegg, An investigation of the determination of serum cholesterol by an enzymatic method, *Ann. Clin. Biochem.* 10 (1973) 79–84.
- [20] M.P. Serrano, M. Vignoni, M.L. Dántola, E. Oliveros, C. Lorente, A.H. Thomas, Emission properties of dihydropterins in aqueous solutions, *Phys. Chem. Chem. Phys.* 13 (2011) 7419–7425.
- [21] Y. Fukunaga, Y. Katsuragi, T. Izumi, F. Sakiyama, Fluorescence characteristics of kynurenine and N'-formylkynurenine, their use as reporters of the environment of tryptophan 62 in hen egg-white lysozyme, *J. Biochem.* 92 (1982) 129–141.
- [22] G.E. Ronsein, M.C.B. Oliveira, S. Miyamoto, M.H.G. Medeiros, P. Di Mascio, Tryptophan oxidation by singlet molecular oxygen [O<sub>2</sub> (1Δg)]: mechanistic studies using 18O-labeled hydroperoxides, mass spectrometry, and light emission measurements, *Chem. Res. Toxicol.* 21 (2008) 1271–1283.
- [23] K.U. Schallreuter, M.A.E.L. Salem, N.C.J. Gibbons, A. Martinez, R. Slominski, J. Lüdemann, H. Rokos, Blunted epidermal l-tryptophan metabolism in vitiligo affects immune response and ROS scavenging by Fenton chemistry, part 1: epidermal H<sub>2</sub>O<sub>2</sub>/ONOO-mediated stress abrogates tryptophan hydroxylase and dopa decarboxylase activities, leading to low serotonin and melatonin levels, *FASEB J.* 26 (2012) 2457–2470.
- [24] J.R. Lakowicz, Principles of Fluorescence Spectroscopy, 3rd ed. Springer, 2006.
- [25] G.S. Harms, S.W. Pauls, J.F. Hedstrom, C.K. Johnson, Fluorescence and rotational dynamics of dityrosine, *J. Fluoresc.* 7 (1997) 283–292.
- [26] H.I. Joschek, S.I. Miller, Photooxidation of phenol, cresols, and dihydroxybenzenes, *J. Am. Chem. Soc.* 88 (1966) 3273–3281.
- [27] T.K. Dalsgaard, J.H. Nielsen, B.E. Brown, N. Stadler, M.J. Davies, Dityrosine, 3,4-dihydroxyphenylalanine (DOPA), and radical formation from tyrosine residues on milk proteins with globular and flexible structures as a result of riboflavin-mediated photo-oxidation, *J. Agric. Food Chem.* 59 (2011) 7939–7947.
- [28] J.W. Heinecke, W. Li, H.L. Daehnke Iii, J.A. Goldstein, Dityrosine, a specific marker of oxidation, is synthesized by the myeloperoxidase-hydrogen peroxide system of human neutrophils and macrophages, *J. Biol. Chem.* 268 (1993) 4069–4077.
- [29] M.S. Kritsky, T.A. Lyudnikova, E.A. Mironov, I.V. Moskaleva, The UV radiation-driven reduction of pterins in aqueous solution, *J. Photochem. Photobiol. B Biol.* 39 (1997) 43–48.
- [30] M.P. Denofrio, P.R. Ogilby, A.H. Thomas, C. Lorente, Selective quenching of triplet excited states of pteridines, *Photochem. Photobiol. Sci.* 13 (2014) 1058–1065.
- [31] F. Wilkinson, H.P. Helman, A.B. Ross, Rate constants for the decay and reactions of the lowest electronically excited singlet state of molecular oxygen in solution, An Expanded and Revised Compilation *J. Chem. Phys. Ref. Data* 24 (1995) 663–667.
- [32] P.R. Ogilby, C.S. Foote, Chemistry of singlet oxygen. 42. Effect of solvent, solvent isotopic substitution, and temperature on the lifetime of singlet molecular oxygen (1Δg), *J. Am. Chem. Soc.* 105 (1983) 3423–3430.
- [33] D.A. Malencik, S.R. Anderson, Dityrosine as a product of oxidative stress and fluorescent probe, *Amino Acids* 25 (2003) 233–247.
- [34] J.D. Spikes, H.R. Shen, P. Kopečková, J. Kopeček, Photodynamic crosslinking of proteins. III. Kinetics of the FMN- and rose bengal-sensitized photooxidation and intermolecular crosslinking of model tyrosine-containing N-(2-hydroxypropyl)methacrylamide copolymers, *Photochem. Photobiol.* 70 (1999) 130–137.
- [35] E.K. Hodgson, I. Fridovich, The role of O<sub>2</sub><sup>-</sup> in the chemiluminescence of luminol, *Photochem. Photobiol.* 18 (1973) 451–455.
- [36] J. Eriksen, C.S. Foote, T.L. Parker, Photosensitized oxygenation of alkenes and sulfides via a non-singlet-oxygen mechanism, *J. Am. Chem. Soc.* 99 (1977) 6455–6456.
- [37] B.H.J. Bielski, D.E. Cabelli, R.L. Arudi, A.B. Ross, Reactivity of HO<sub>2</sub>/O<sup>-</sup> 2 radicals in aqueous solution, *J. Phys. Chem. Ref. Data* 14 (1985) 1041–1100.
- [38] I. Fridovich, Superoxide radicals, superoxide dismutases and the aerobic lifestyle, *Photochem. Photobiol.* 28 (1978) 733–741.